International Journal of Engineering and Technology Research
Vol. 1, No. 8, September 2013, PP: 136-144, ISSN: 2327-0349 (Online)
Available online at www.ijeatr.org

Research article

SEISMIC EVALUATION of LOW STRENGTH CONCRETE MEMBERS of EXISTING BUILDINGS in JAPAN

Kubilay Kaptan

Disaster Education, Application and Research Center, Istanbul Aydin University
E-mail: kubilaykaptan@aydin.edu.tr

ABSTRACT

This study reports on 10 RC columns with LSC of 5, 10 N/mm^2 grade. The test variables were the strength of concrete, different main reinforcement and retrofitting or not. The test specimens with round main reinforcements did not brake with shear failure due to little bond strength of the main reinforcements, and a state of the shear compressive failure by the slippage compressive failure on the diagonal of the concrete appears conspicuously. Therefore the relationship between shear and the lateral displacement angle showed a property of ductility without the yield strength deterioration to 0.032 rad after maximum load although it almost showed the hysteresis curve of a remarkable reverse S-shaped. The maximum strength obtained from the plastic theory considering of the truss mechanism allowed for bond strength and the arch mechanism based on local bearing strength. In conclusion, even columns with LSC have the performance as columns and can be retrofitted.

Keywords: Low Strength Concrete, Shear Strength, Existing Buildings, Seismic Evaluation, Seismic Retrofit

---

1. INTRODUCTION

Seismic diagnosis and seismic retrofit of existing buildings are performed in Japan, and a lot of existing RC buildings of low compressive strength concrete which less than 13.5 N/mm^2 (hereinafter referred to as LSC) were found. It is important to research on LSC because the Japanese standard of seismic diagnosis and retrofit is not applied to LSC. Compared to the amount of research on normal and high compressive strength concrete, few studies indeed have been done to analyze LSC. Thus little is known about characters of material and members of LSC. For above reason, Authors organized the committee on low strength concrete in the Chugoku branch of Japan Concrete Institute, this would be the first committee that experimental studies were pushed forward about LSC systematically. This paper reports on 10 of 36 test specimens in the above committee and the effect of retrofit with carbon fiber reinforced plastics (CFRP) for LSC columns.

2. OUTLINE OF TESTS

2.1. Test Variable

10 test specimens with LSC of 5 and 10 N/mm^2 were built, as illustrated in **Figure 1**. The test variable is concrete strength, axial force ratio, tension reinforcement ratio, layer of carbon fiber sheet (CF sheet) and shear reinforcement ratio, shown as **Table 1**. 4 of 10 test specimens were non-retrofitted and other 6 test specimens were retrofitted with CFRP. The shear reinforcements in all test specimens were arranged with 2-D6 and 100mm of each shear reinforcements interval in **Figure 1**, and shear reinforcement ratio was p_w =0.21%. All test specimens were planned to break by shear failure. One of the characteristics on this study is to be tested with working higher axial load than usual. The reason why such high axial force ratio is chosen is that even though same axial force, as the compressive strength of concrete becomes lower, the axial force ratio becomes higher. Other characteristic is the round steel bars are used as main reinforcements because the existing school buildings before 1965 were built with round steel bars as main reinforcements.

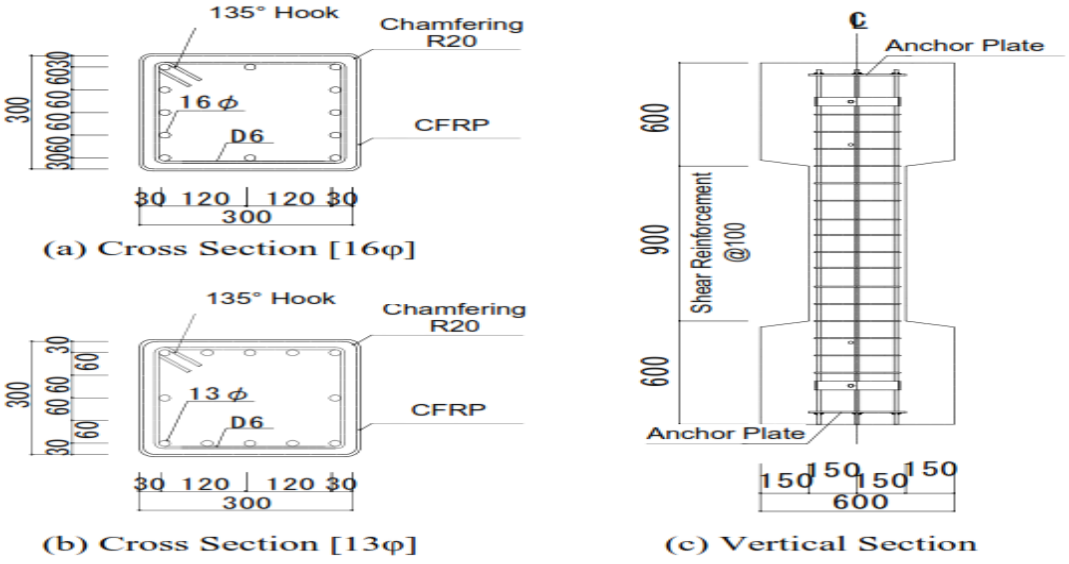

Figure 1: Dimension and Shape of Test Specimens [unit: mm]

Table 1: Outline of Tests

No.	Name of Specimens	σ_B [N/mm^2]	Main Reinforcement	n	Layer of CF Sheet	p_w [%]
8	L10240	13.50	16φ	0.4	none	1.12
12	DL10240	13.89	D16			1.11
30	L05280S	4.69	13φ	0.8		0.74
32	L10280S	10.56				
13	L1024C1	9.55	16φ	0.4	0.5	1.12
14	L1024C2	9.60			2	
15	DL1024C1	9.67	D16		0.5	1.11
16	DL1024C2	9.74			2	
33	L0528C2S	4.62	13φ	0.8	2	0.74
34	L1028C2S	10.56				

σ_B; Compressive Strength of Concrete, n; Axial Force Ratio $n = N/(b \cdot D \cdot \sigma_B)$, N; Axial Force [N], b; 300 [mm], D;300 [mm], CF Sheet; 200 [g/m^2]

The loading rule experimented on by 0.2×10^{-2} rad. by the same displacement amplitude to 3.2×10^{-2} rad. twice. The axial force on test specimens was worked before working the horizontal load. Test specimens were always worked constant axial force while testing.

2.2. Materials

Table 2 presents the mix proportion of LSC, stress-strain curves of concrete appears in **Figure 2**. The notable feature of LSC is it has very ductile. **Table 3** shows the characteristics of main reinforcement (φ13 and φ16) and shear reinforcement (D6). **Figure 2** appears the stress-strain curves of main and shear reinforcement and CF sheet and picture of the CF sheet.

Table 2: Mix Proportion of Low Strength Concrete

Specified Design Strength [N/mm^2]	5	10
Water [kg/m^3]	210	210
Sand Percentage [%]	49.9	50.2
Water/Binder Ratio [%]	65.0	65.0
Water/Cement Ratio [%]	221.0	122.0

Table 3: Tensile Test Result of Steel Reinforcement

Kind of Main Reinforcement	Yield Strength [N/mm^2]	Young's Modulus [N/mm^2]
16φ	340	1.88×10^5
D16	372	1.77×10^5
13φ	320	2.01×10^5
D6	320	1.92×10^5

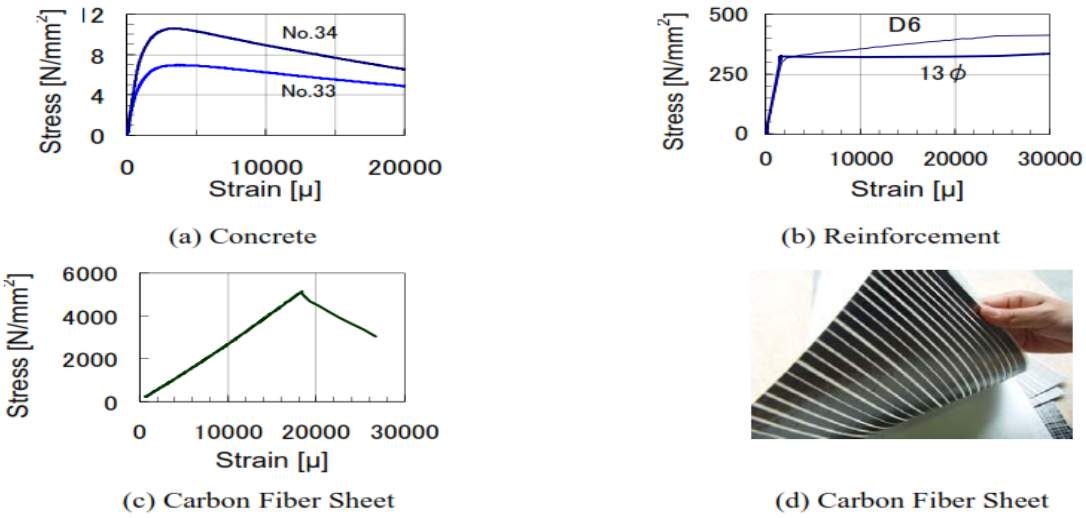

Figure 2: Materials

International Journal of Engineering and Technology Research
Vol. 1, No. 8, September 2013, PP: 136-144, ISSN: 2327-0349 (Online)
Available online at www.ijeatr.org

3. TEST RESULTS

Figure 3 illustrates hysteresis curves and **Figure 4** illustrates envelope curves, the dashed lines on curves show the calculated overturning moment value. Four test specimens are non-retrofitted columns, as illustrated in **Figure 3** (a)-(d), the others are retrofitted columns. Three test specimens are columns built with deformed bar as main reinforcement, as illustrated in **Figure 3** (b), (g) and (h), and the others are built with round bars. The hysteresis curves of columns with LSC tend to show more ductile behavior than columns with normal strength concrete, regardless of experimental variables. To put it more concretely, a few characteristics are shown on kind of main reinforcements, differences of layers of CF sheet or axial force ratio. Compared the hysteresis curves of different kinds of main reinforcements as the first characteristic, the strength of columns with deformed bars as main reinforcements suddenly decreases after maximum strength. On the other hand, the strength of columns with round bars as main reinforcements pretty gently or hardly decreases. Though the characteristic is shown regardless of retrofitted or non-retrofitted test specimens, it is clearer on non-retrofit test specimens.

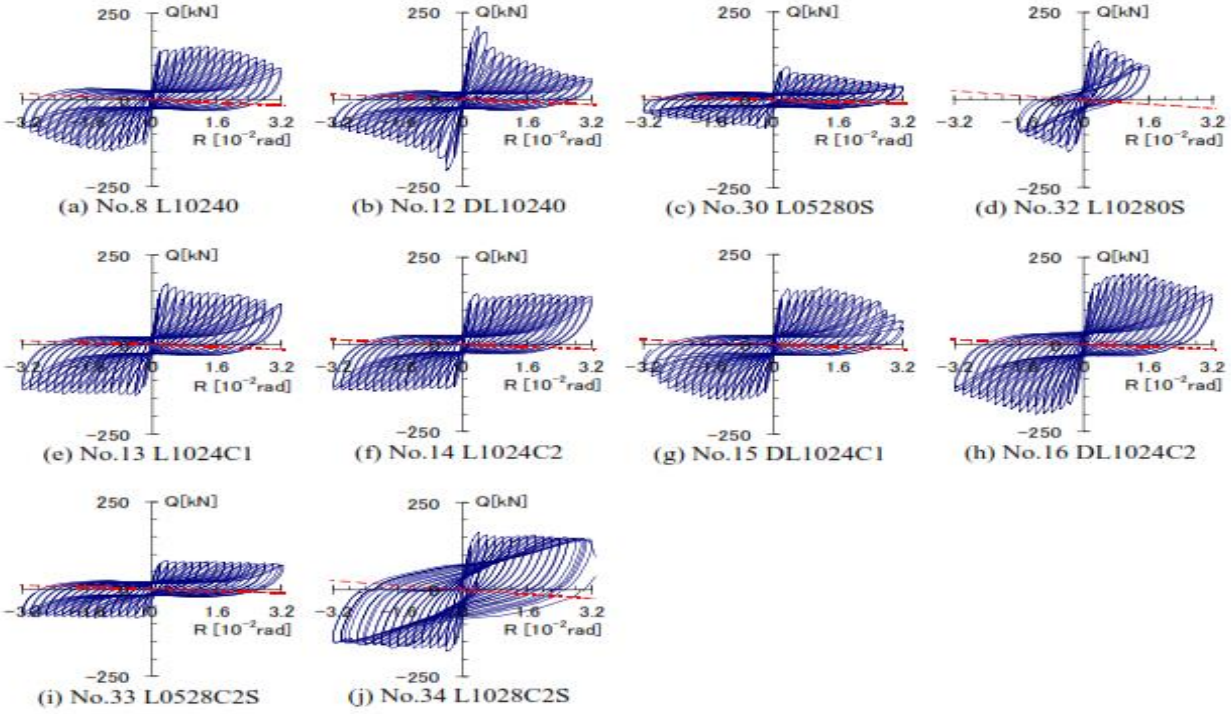

Figure 3: Hysteresis Curves

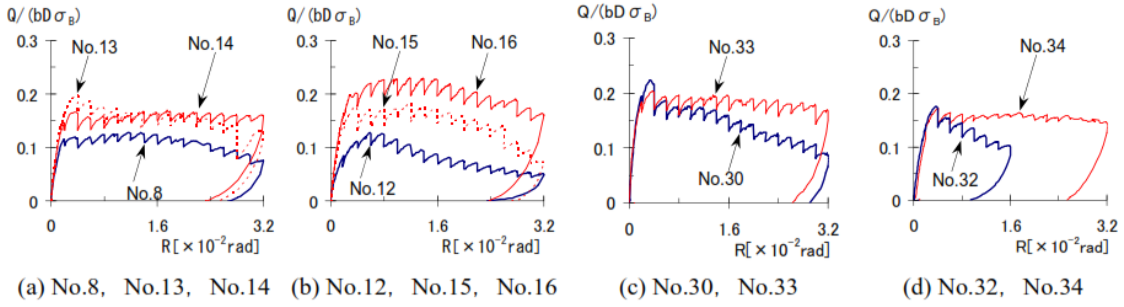

Figure 4: Envelope Curves

It is the second characteristic that the hysteresis curves show that the strength of columns with round bars as main reinforcement hardly decreasing even on non-retrofit column. Such tendency shows the stronger on the column retrofitted with the more layers within the narrow limits of two layers. The third characteristic is retrofit of CFRP is especially effective to the column with high axial force ratio and deformed bars as main reinforcements. This seismic retrofit theory is effective for even LSC columns.

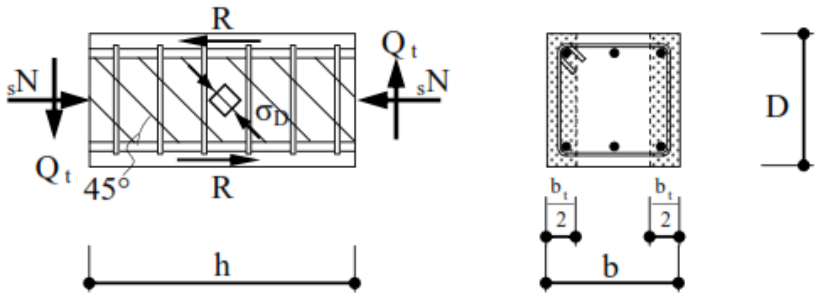

Figure 5: Truss Mechanism with Bond Splitting Failure

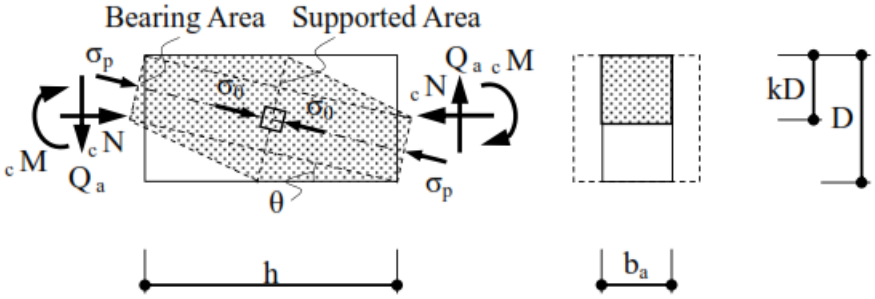

Figure 6: Arch Mechanism in Local Compressive Field

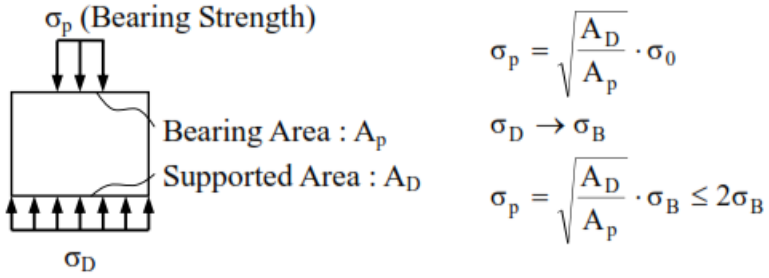

Figure 7: Bearing Strength

4. ULTIMATE SHEAR STRENGTH BY PLASTIC THEORY

The evaluation of the ultimate shear strength of LSC columns calculates by the plastic theory based on Architectual Institute of Japan (1990). The plastic theory allows the mixed model of the truss mechanism and arch mechanism as the shear resistance mechanism. The strength of the truss mechanism is decided by the bond strength on main reinforcement as illustrated in **Figure 5**. Assuming that the angle of inclination of the unyield shear reinforcement is 45° for transmitting the bond strength, the concrete compressive strength σ_B is kept in the concrete compressive field in **Figure 5**. Then Q_{Ut}, the ultimate shear strength of the bond strength, is evaluated by Eqn. 4.1.

$$Q_{Ut} = \tau_{Ub}.\sum \varphi.D \quad (4.1)$$

where, $\tau_{Ub} = \frac{\varepsilon.A.E}{l.\varphi}$ (4.2)

ε: strain of main reinforcement, A: area of main reinforcement [mm^2],
E: Young's modulus [N/mm^2], *l*: bond splitting length [mm],
φ: perimeter of longitudinal reinforcement [mm]

in addition, for establishing the mechanism, the width b_t of concrete compressive field is given by Eqn. 4.3.

$$b_t = 2.\frac{\tau_{Ub}}{\sigma_B}.\sum \varphi \quad (4.3)$$

It is assumed that the arch mechanism as illustrated in **Figure 6** is constituted when the resultant uniaxial compressive stress, σ_o, of the normal stress, σ_p, both uniformly distributed over the compression region at both ends of the reinforcement-less concrete with the width b_a, which is the remaining width used for the arch mechanism and given by Eqn. 4.4, are produced in the direction that is off from the member axis by the angle of θ. Further, the maximum shear resistance of the arch mechanism is assumed to take place when the above-mentioned resultant stress, σ_0, reaches σ_p when the shear strength, Q_{Ual}, can be expressed by Eqn. 4.5.

$$b_a = b - b_t \quad (4.4)$$

$$Q_{Ual} = \left[\sqrt{4 + \left(\frac{\eta}{c^{n_0}}\right)^2 - 4_c n_0^2} - \left(\frac{\eta}{c^{n_0}}\right)\right].\frac{b_a.D.\sigma_B}{2} \quad (4.5)$$

Where, η=h/D (4.6)

$$c^{n_0} = \sqrt{\frac{\sqrt[3]{\eta^2+\eta^2\sqrt{1+\eta^2}}}{2} + \frac{\sqrt[3]{\eta^2-\eta^2\sqrt{1+\eta^2}}}{2}} \quad (4.7)$$

The Q_{sU2} is given by superposition of Q_{Ut} and Q_{Ual} by Eqn. 4.8. Furthermore, the confined effect for concrete is evaluated by Eqn. 4.9. Chan (1955) suggests 2.05 as the coefficient of column with square cross section in Eqn. 4.10, this coefficient is half of the coefficient for circular cross section by the research of Richart, Brandtzaeg and Brown (1929). The result of our experiment shows that it is reasonable to apply these coefficients to LSC (See Appendix)

$$\acute{\sigma}_B = \lambda.\sigma_B \quad (4.9)$$

where, $\lambda = 1 + 2.05\frac{P_W.\xi_P.\sigma_{wy}}{\sigma_B}$ (4.10)

Let σ'_B be σ_B in Eqn. 4.5, the strength of the arch mechanism considered the confined effective for concrete is given by Eqn. 4.11. (See **Figure 6** and **Figure 7**)

$Q_{ua2}=\lambda.Q_{Ual}$ (4.11)

Then, the ultimate shear strength Q_{sU3} is given by superposition Q_{Ut}, and Q_{ua2} by Eqn. 4.12.

$Q_{sU3}=Q_{Ut} + Q_{ua2}$ (4.12)

All calculated ultimate shear strength are shown on Table 4 and According to **Figure 8**, calculated ultimate shear strength by Eqn. 4.12 agrees the experimental results.

Table 4: Ultimate Shear Strength

No.	Name of Specimens	σ_B [N/mm^2]	τ_{Ub} [N/mm^2]	λ	Experimental Strength		Calculated Ultimate Shear Strength		
					Positive	Negative			
					Q_{sU0} [kN]	Q_{sU0} [kN]	Q_{sU1} [kN]	Q_{sU2} [kN]	Q_{sU3} [kN]
8	L10240	13.50	1.22	1.09	160.8	154.0	152.2	202.6	214.0
12	DL10240	13.89	2.08	1.09	212.5	206.6	156.6	225.1	235.8
30	L05280S	4.69	0.42	1.30	95.0	83.6	52.9	67.1	80.8
32	L10280S	10.56	0.95	1.13	170.6	152.8	119.1	151.1	164.8
13	L1024C1	9.55	0.86	1.25	171.4	143.2	107.7	143.3	166.4
14	L1024C2	9.60	0.86	1.63	154.4	141.4	108.3	144.1	202.2
15	DL1024C1	9.67	1.83	1.25	164.8	161.6	109.1	169.5	189.8
16	DL1024C2	9.74	2.14	1.62	206.7	206.1	109.9	180.5	228.9
33	L0528C2S	4.62	0.42	2.36	84.2	83.1	52.1	66.1	128.1
34	L0528C2S	10.56	0.95	1.59	168.0	179.9	119.1	151.1	213.1

Figure 8: Comparison of experimental value with calculated value

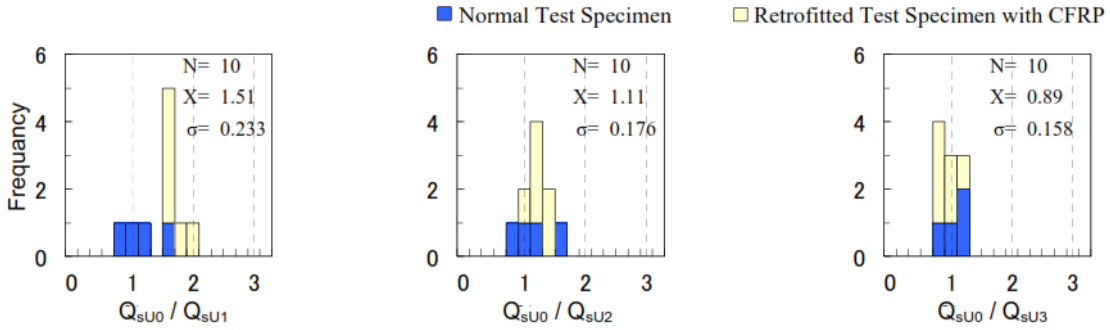

5. CONCLUSIONS

The following results were obtained in this paper:

1. Even if the column with LSC of 5 N/mm^2 grade and round bars as main reinforcements, it was able to perform cyclic load to the displacement amplitude of 3.2x10^{-2} rad., did not finally occur the decreased strength.
2. The ultimate shear strength is able to evaluate by the plastic theory, however it is necessary to further examine the quantification of the confined effect.
3. Even columns with LSC have the performance as columns and can be retrofitted by carbon fiber sheet (CFRP).

REFERENCES

[1] Chan, W. W. L. (1955) The Ultimate Strength and Deformation of Plastic Hinges in Reinforced Concrete Frameworks, Magazine of Concrete Research, 7:21, 121 - 132.

[2] Richart, F. E., Brandtzaeg, A. and Brown, R. L. (1929). The Failure of Plain and Spirally Reinforced Concrete in Compression. Engineering Experiment Station. University of Illinois Bulletin, 26:31.

[3] The Architectural Institute of Japan (1990). Design Guideline for Earthquake Resistant Reinforced Concrete Buildings Based on Ultimate Strength Concept, Architectural Institute of Japan, Japan (in Japanese)

[4] The Japan Building Disaster Prevension Association (2001). Seismic Evaluation Standard for Existing Reinforced Concrete Structure, Japan, (in Japanese)

[5] The Special Research Committee on the Low Strength Concrete of the Chugoku Branch of Japan Concrete Institute. (2009). The Research Report on Special Research Committee on the Low Strength Concrete. (in Japanese)
Wakabayashi, Minoru. and Minami, Koichi. (1979). Some Tests on the Method to Prevent Shear Failure in Reinforced Concrete Columns.

[6] Annuals of Desaster Prevention Research Institute, Kyoto University, Vol. 22: B-1, 295-316., (in Japanese)

International Journal of Engineering and Technology Research
Vol. 1, No. 8, September 2013, PP: 136-144, ISSN: 2327-0349 (Online)
Available online at www.ijeatr.org

APPENDIX

The effect of retrofit of CFRP is supported by some experimental for LSC. Table A1 and Figure A1 shows the experimental results.

Table A1: Experimental variable

Series	I				II				III			
Shape	Circular Cylinder				Circular Cylinder				Prismatic Column			
Size	100φ×200				150φ×300				150×150×300			
Layer of CF Sheet	0	0.5	1.0	2.0	0	0.5	1.0	2.0	0	0.5	1.0	2.0
$p_{w(CF)}$ [%]	0.00	0.11	0.22	0.44	0.00	0.07	0.15	0.30	0.00	0.07	0.15	0.30
$p_{w(CF)} \cdot \sigma_{w(CF)}$ [N/mm^2]	0.11	1.79	3.57	7.15	0.00	1.19	2.38	4.77	0.00	1.19	2.38	4.77
σ_B [N/mm^2]	8.81	20.18	30.19	49.38	8.01	16.04	25.66	38.53	7.47	11.82	14.87	18.14

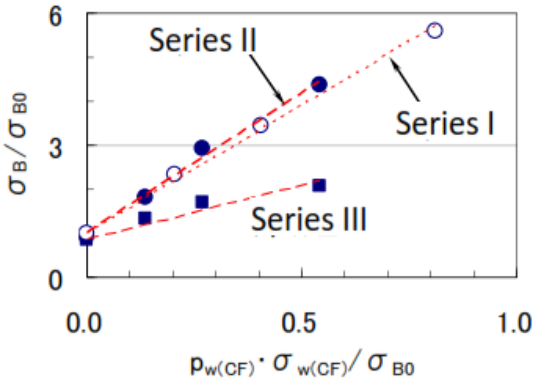

Figure A1: Relationship between $P_{w(CF)}.\sigma_{w(CF)} / \sigma_{B0}$ and σ_B / σ_{B0}

These results lead Eqn. A1-A3 and agree the results by Richart, Brandtzaeg and Brown (1929) and Chan (1955).

$$Series\ I: \frac{\sigma_B}{\sigma_{B0}} = 1 + 5.7778 \frac{P_{w(CF)} \cdot \sigma_{w(CF)}}{\sigma_{B0}} \quad \text{(A1)}$$

$$Series\ II: \frac{\sigma_B}{\sigma_{B0}} = 0.91 + 6.6095 \frac{P_{w(CF)} \cdot \sigma_{w(CF)}}{\sigma_{B0}} \quad \text{(A2)}$$

$$Series\ III: \frac{\sigma_B}{\sigma_{B0}} = 0.85 + 2.4664 \frac{P_{w(CF)} \cdot \sigma_{w(CF)}}{\sigma_{B0}} \quad \text{(A3)}$$